7678 *Macromolecules* **2009**, *42*, 7678–7688
DOI: 10.1021/ma900879f

Macromolecules
ARTICLE

Long-Range Chirality Transfer in Free Radical Polymerization of Bulky Vinyl Monomers Containing Laterally Attached *p*-Terphenyl Groups

Jiaxi Cui, Xiaocun Lu, Anhua Liu, Xinhua Wan,* and Qifeng Zhou

Beijing National Laboratory for Molecular Sciences, Key Laboratory of Polymer Chemistry and Physics of Ministry of Education, College of Chemistry and Molecular Engineering, Peking University, Beijing 100871, China

Received April 22, 2009; Revised Manuscript Received August 18, 2009

ABSTRACT: Two series of chiral bulky vinyl monomers, 2-(4′-hexyloxyphenyl)-5-(4′-alkoxycarbonylphenyl)styrene and 2-(4′-alkoxycarbonylphenyl)-5-(4′-hexyloxyphenyl)styrene (abbreviated as ***S*-(+)-HexM*m***/***R*-(−)-HexM0** and ***S*-(+)-M*m*Hex/*R*-(−)-M0Hex** (m = 0, 1, 2, 3), respectively), were designed and synthesized. The former differed the latter only by the relative location of vinyl group, i.e., orientation against or toward the stereocenter. Except for ***S*-(+)-HexM1** and ***S*-(+)-HexM3**, all the monomers readily underwent radical polymerization to yield the polymers displaying optical rotations and Cotton effects in the UV−vis absorption region of side groups distinct to the corresponding model compounds and mononmers, implying the formation of main chain chirality, most probable helicity. The influences of the configuration, the distance to *p*-terphenyl, and the position relative to vinyl group of stereocenter on the chiroptical properties of the resultant polymers were systematically studied. It was found that inverting the absolute spatial configuration of asymmetric center or changing the parity of methylene number between stereocenter and *p*-terphenyl alternated the direction of optical rotation of polymer, similar to the odd−even alternation behavior observed in the cholesteric phase of achiral 2,5-bis(4′-hexyloxyphenyl)styrene doped with the corresponding monomers. This parallel indicated an identical driving force for the formation of chiral mesophase and the asymmetric secondary structure of the polymer. When the spatial configuration of stereocenter was fixed, its distance to *p*-terphenyl rather than vinyl group played a dominant role in the induction of an excess helical sense. However, the stereogenic center at the ortho position of vinyl group exhibited a larger induction power than those at the meta position.

Introduction

One of the important topics in polymer chemistry is facile synthesis of optically active helical polymers because these materials are not only of great interest in asymmetric synthesis, molecular recognition, and photoelectrical materials, but also favorable models to understand how complex chiral bioarchitecture is built up from primary molecular blocks.[1−5] Optically active helical polymer can be obtained from either achiral monomer through asymmetric polymerization initiated by chiral initiator or chiral, nonracemic monomer, the stereocenter of which supplies a bias to induce a prevailing helical sense.[6−17] With the latter approach, the chiral atom is preferred to be connected directly or as closely as it can with the polymerizable group in order to increase the asymmetric coupling between side group and polymer backbone.[9b] Insertion of rigid spacer between polymerizable group and stereogenic center has been known to help chiral teleinduction during polymerization.[18] For example, in a series of chiral promesogenic isocyanides developed by Serrano, Veciana, and co-workers, the stereocenters pass their chiral information to the growing main-chains over the distance of at least 14 covalent bonds by virtue of the noncovalent steric interaction of rigid phenyl benzoate spacer.[18a,b] More remarkably, the sense of helical induction follows an odd−even alternation rule when the stereocenter in chiral tail is away from the mesogenic core, as found in the induction of twisting mesophase of low molecular mass liquid crystals.[18b] Afterward, the influences of the length, constitution and conformation of stiffened spacer between an isocyanide group and a chiral substituent on the diastereoselectivity of polymerization were also addressed.[18e,g] However, Masuda and co-workers found only one polymer showed weak positive optical rotation ($[R]_D$ +4°) and all the other four displayed strong negative optical rotations ($[R]_D$ −340° to −612°) in a series of helical poly(propiolic ester)s with chiral moieties that possessed identical stereogenic centers, but different numbers of methylene groups between the ester group and asymmetric atom.[19] The similar odd−even effects have also been investigated in chiral polythiophene,[20] polysilylene aggregates,[15e] polyfluorenes, and poly-*p*-phenylenevinylene in bulk.[21] Despite these numerous studies, little has been known about the chiral teleinduction of vinyl monomer in polymerization, especially in radical polymerization.

Recently, we described for the first time the odd−even effect in free radical polymerization of optically active 2,5-bis[(4′-alkoxycarbonyl)phenyl]styrene (***S*-(+)-M*m*/*R*-(−)-M0**, m = 0, 1, 2, 3; Chart 1).[22] The chiral carbon atoms in the alkoxy groups were

Chart 1. Chemical Structures of *S*-(+)-M*m*/*R*-(−)-M0

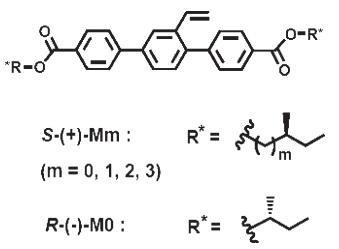

*Corresponding author. Telephone: 86-10-62754187. Fax: 86-10-62751708. E-mail: xhwan@pku.edu.cn.

 Published on Web 09/08/2009

found to transmit their chiralities to the propagating polymer main chain over long distance during polymerization. Inverting the spatial configuration of asymmetric center or changing the parity of covalent bond number between stereocenter and *p*-terphenyl group changed the sense of the optical rotation of the polymer in an alternate way. This observation paralleled the dependence of the helical twist sense of the chiral nematic phase of achiral 2,5-bis(4′-hexyloxyphenyl)styrene (**BHPSt**) induced by the corresponding chiral monomers, indicating the same driving force for the formation of chiral mesophase and the chiral secondary structure of the polymer. However, unlike promesogenic isocyanides mentioned above, which contain only a single stereogenic atom, each molecule in these bulky vinyl monomers had two stereocenters, the distance of them relative to *p*-terphenyl core and vinyl group was not same. Should the distance between stereocenter and *p*-terphenyl group play a dominant role in the induction of helicity, the two stereogenic centers would act collaboratively. Otherwise, their contributions would counteract. Furthermore, the rotation barriers around the C−C bonds linking the phenyl rings were different and therefore should influence the chirality transfer from the stereogenic center in the terminal of side chain into the polymer main chain. However, the previous work did not give any answer on these concerns.

Herein, we report synthesis and radical polymerization of novel chiral bulky vinyl monomers, 2-(4′-hexyloxyphenyl)-5-(4′-alkoxycarbonylphenyl)styrene and 2-(4′-alkoxycarbonylphenyl)-5-(4′-hexyloxyphenyl)styrene. The two types of molecules are abbreviated as ***S***-(+)-**HexM*m*/*R*-(−)-HexM0** and ***S***-(+)-**M*m*Hex/*R*-(−)-M0Hex** (m = 0, 1, 2, 3), respectively (where ***S*** and ***R*** represent absolute spatial configuration of stereocenter; **M** and **P** imply monomer and polymer, respectively; ***m*** indicates the number of methylene groups between the stereocenter and the ester group; **Hex** means the hexyloxy terminal of side-group and denotes a monomer with vinyl group oriented against chiral alkoxy group when it is placed before **P** or **M**). The latter group distinguishes the former only by the orientation of vinyl group with respect to the stereocenter, i.e. against or toward the stereocenter. They are similar in structures to the previously reported monomers ***S***-(+)-**M*m*/*R*-(−)-M0** but with only a single stereogenic center. They are designed mainly for two reasons. First, the distance from chiral atom to *p*-terphenyl was same for both ***S***-(+)-**HexM*m*/*R*-(−)-HexM0** and ***S***-(+)-**M*m*Hex/*R*-(−)-M0Hex**. Whereas, the distance from chiral atom to vinyl group of ***S***-(+)-**HexM*m*/*R*-(−)-HexM0** is one convalent bond longer than ***S***-(+)-**M*m*Hex/*R*-(−)-M0Hex**. Such a minor structural modification is expected to help us to identify which distance exerts a dominant effect on the diastereoselectivity during the formation of helical polymer backbone. Second, the population of various rotamers of ***S***-(+)-**HexM*m*/*R*-(−)-HexM0** is different from that of ***S***-(+)-**M*m*Hex/*R*-(−)-M0Hex**, which should remarkably affect the chirality transfer from the stereocenter of monomer to growing polymer backbone. The chiroptical properties of the corresponding polymers are characterized by polarimetry and circular dichroism spectroscopy (CD). Liquid crystal induced circular dichroism (LCICD) technique is applied to understand the role governing the long-range chirality transfer in free radical polymerization of these monomers.[23]

Results and Discussion

Monomer and Polymer Syntheses. The two series of chiral monomers, ***S***-(+)-**HexM*m*/*R*-(−)-HexM0** and ***S***-(+)-**M*m*Hex/*R*-(−)-M0Hex**, were prepared via multistep synthetic routes as illuminated in Schemes 1 and 2. The synthesis began with 2-iodo-5-bromotoluene. Owing to the different reactivities of bromine and iodine toward Suzuki cross-coupling reaction, this compound was converted to 2-(4′-hexyloxyphenyl)-5-bromotoluene and 2-(4′-methoxycarbonylphenyl)-5-bromotoluene by reaction with 4-hexyloxyphenylboronic acid and 4-methoxycarbonylphenylboronic acid, respectively. Bromination of biphenyl compounds with *N*-bromosuccinimide, followed by the reactions with triphenylphosphine, yielded (2-(4′-hexyloxyphenyl)-5-bromobenzyl)triphenylphosphonium bromide and (2-(4′-methoxycarbonylphenyl)-5-bromobenzyl)triphenylphosphonium bromide, separately. The Wittig reaction of the phosphonium salts with formaldehyde in aqueous solution under alkaline condition produced 2-(4′-hexyloxyphenyl)-5-bromostyrene and 2-(4′-methoxycarbonylphenyl)-5-bromostyrene. Further Suzuki coupling reaction with 4-methoxycarbonylphenylboronic acid or 4-hexyloxyphenylboronic acid, followed by the hydrolysis in aqueous sodium hydroxide solution, resulted in 2-(4′-hexyloxyphenyl)-5-(4′-carboxylphenyl)styrene and 2-(4′-carboxyphenyl)-5-(4′-hexyloxylphenyl)styrene, separately. The acid was first acylated by oxalyl chloride and then reacted with chiral alcohols to give the target molecules, ***S***-(+)-**HexM*m*/*R*-(−)-HexM0** and

Scheme 1. Syntheses of Monomers *S*-(+)-HexM*m*/*R*-(−)-HexM0 and Their Corresponding Polymers *S*-(+)-HexPm/*R*-(−)-HexP0

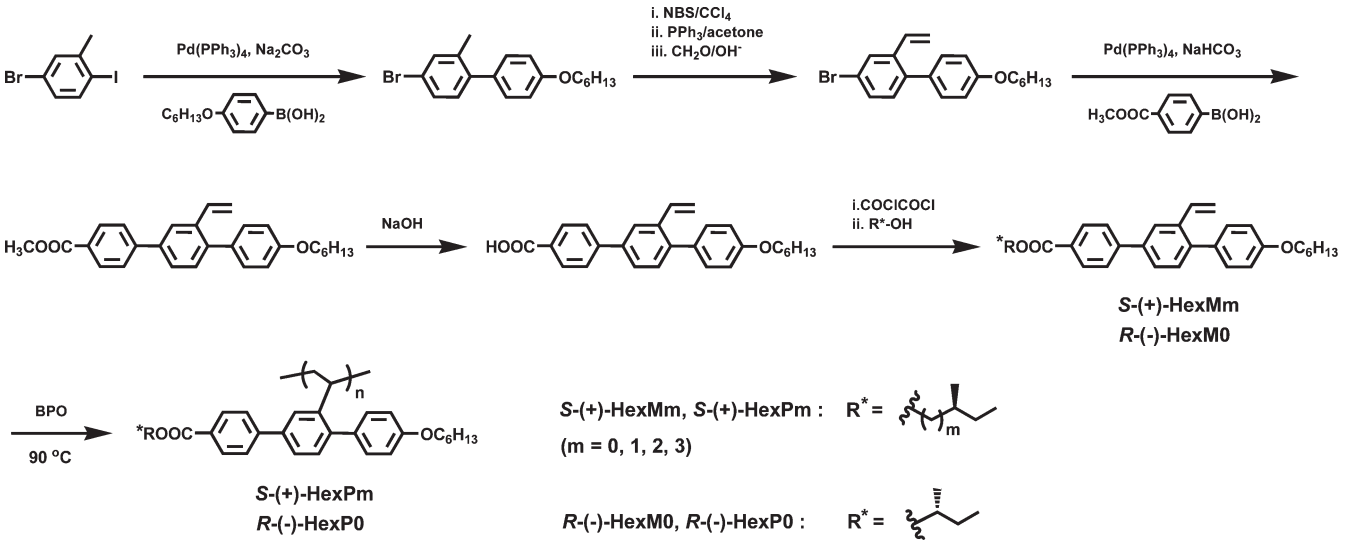

Scheme 2. Syntheses of Monomers *S*-(+)-M*m*Hex/*R*-(−)-M0Hex and Their Corresponding Polymers *S*-(+)-PmHex/*R*-(−)-P0Hex

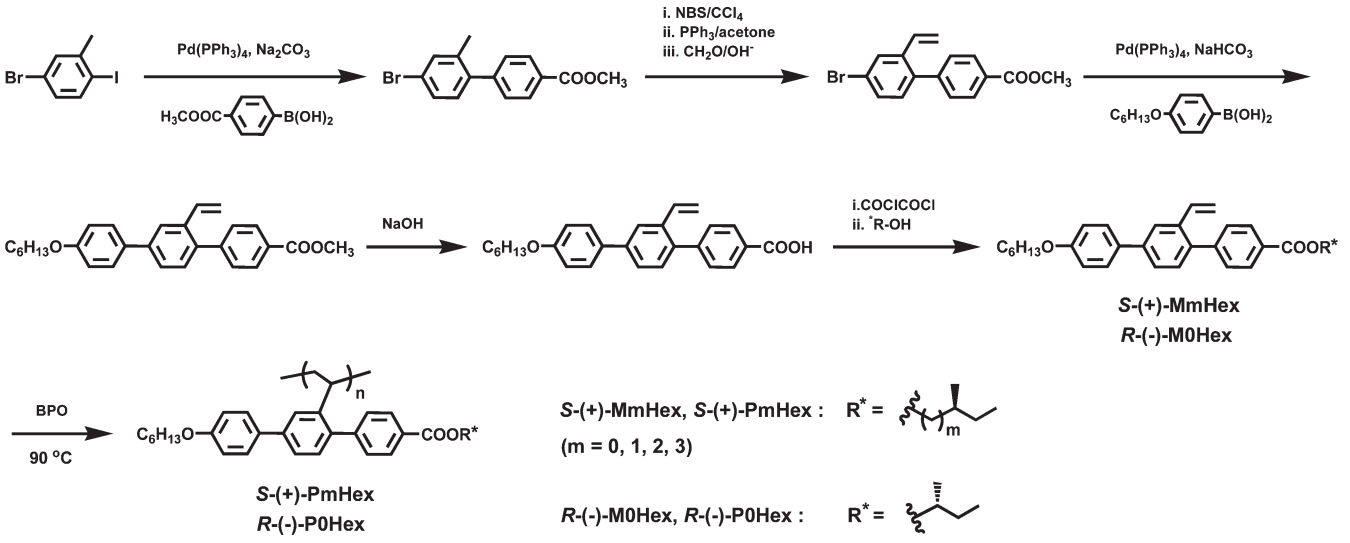

Chart 2. Chemical Structures of Model Compounds *S*-(+)-ImHex/*R*-(−)-I0Hex and *S*-(+)-HexIm/R-(−)-HexI0[a]

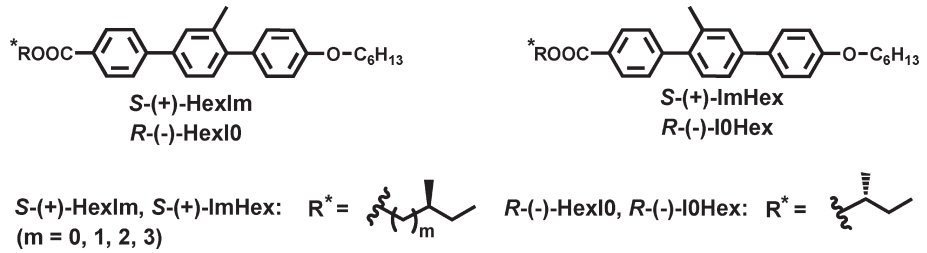

[a] The abbreviations have the meanings identical to those of monomers and polymers except **I** denotes model compound.

***S*-(+)-M*m*Hex/*R*-(−)-M0Hex**. Their absolute configurations were predetermined by the reaction route through which they were prepared from the alcohols with known absolute configurations.

The model compounds, ***S*-(+)-ImHex/*R*-(−)-I0Hex** and ***S*-(+)-HexIm/*R*-(−)-HexI0** (Chart 2), were prepared with a similar method. The structures of intermediates, model compounds and monomers were characterized by proton NMR, mass spectrometry, and elementary analysis. All the data agreed well with the expected structures.

Radical polymerization was carried out in anisole solution at 90 °C using benzoyl peroxide as an initiator. The reaction condition was chosen since they had been proved to yield polymers with high optical rotations for a number of monomers with similar structures.[22,24] As summarized in Table 1, all the monomers were converted to the corresponding polymers with moderately high molecular weights [(5.2−13.2) × 10^4 Da] in good to excellent yields (>80%). These polymers had good solubilities in many organic solvents such as tetrahydrofuran (THF), chloroform, anisole, and heptane.

Chiroptical Properties. The chiroptical properties of model compounds, monomers and the corresponding polymers are summarized in Table 2. The monomers and model compounds containing stereogenic centers with ***S*** configuration displayed positive optical rotations in THF. The specific optical rotations ($[\alpha]_{365}^{25}$) of monomers were comparable to those of the model compounds, suggesting that the reaction at vinyl group did not influence the optical properties of such molecules significantly. However, after polymerization, all the resultant polymers except for ***S*-(+)-HexP1** and ***S*-(+)-HexP3** showed optical rotations quite different from those of the corresponding monomers and model compounds. For example, ***S*-(+)-HexP0** had an $[\alpha]_{365}^{25}$ value of −233.2° (*c* = 5 mg/mL, THF), while that of ***S*-(+)-HexM0** was 84.4°. The opposite sign of optical rotation of ***S*-(+)-HexP0** to its monomer and a large increase in magnitude indicated that the optical activity of polymer did not solely arise from the configurational chirality in the side group and that a higher chiral structure, most likely secondary helical structure of main chain for a vinyl polymer like ***S*-(+)-HexP0**, had been formed. Changing the configuration of stereocenter from *S* to *R* as in ***R*-(−)-HexM0** and ***R*-(−)-HexP0** led to an inversion of the sign of optical rotations for both monomer and polymer, suggesting the remarkable role of the stereocenter in the induction of a prevailing helical sense.

Circular dichroism spectroscopy was used to further characterize the structures of polymers. Figure 1 presents the UV−vis absorption and CD spectra of ***R*-(−)-HexI0**, ***R*-(−)-HexM0**, and ***R*-(−)-HexP0**. The monomer ***R*-(−)-HexM0** revealed an absorption peak centered at 296 nm and a shoulder at 260 nm, which were assigned as the electronic transitions of side *p*-terphenyl and vinyl groups, separately.[25] Its CD spectrum exhibited only very weak Cotton effects in the same region. After polymerization, the absorption of vinyl group disappeared completely and only an absorption peak at 296 nm was observed. The CD spectrum of ***R*-(−)-HexP0** showed two intensive positive Cotton effects centered at 258 and 308 nm, respectively, implying the side *p*-terphenyl groups were arranged in a

Table 1. Polymerization Results of Chiral Bulky Vinyl Monomers

monomer	polymer	yield (%)	$M_n \times 10^{-4}$ [a]	M_w/M_n [a]	T_g (°C) [b]	T_d (°C) [c]
***R*-(−)-HexM0**	***R*-(−)-HexP0**	92	5.2	1.47	156	327
***S*-(+)-HexM0**	***S*-(+)-HexP0**	80	7.4	1.31	155	327
***S*-(+)-HexM1**	***S*-(+)-HexP1**	87	9.9	1.30	160	337
***S*-(+)-HexM2**	***S*-(+)-HexP2**	88	11.2	1.56	161	340
***S*-(+)-HexM3**	***S*-(+)-HexP3**	80	8.1	1.29	147	361
***R*-(−)-M0Hex**	***R*-(−)-P0Hex**	91	9.3	1.63	160	329
***S*-(+)-M0Hex**	***S*-(+)-P0Hex**	84	14.4	1.45	158	329
***S*-(+)-M1Hex**	***S*-(+)-P1Hex**	81	13.2	1.58	141	339
***S*-(+)-M2Hex**	***S*-(+)-P2Hex**	86	10.2	1.71	136	354
***S*-(+)-M3Hex**	***S*-(+)-P3Hex**	85	12.0	1.58	134	370

[a] Number-average molecular weight (M_n), weight-average molecular weight (M_w) and polydispersity (M_w/M_n) were determined by GPC in THF on the basis of standard polystyrene calibration. [b] Glass transition temperature. [c] Temperature at which 5% weight loss was observed under N_2.

Table 2. Chiroptical Properties of Model Compounds, Monomers, Polymers, and Cholesteric Phases of 2,5-Bis(4′-hexyloxycarbonylphenyl)-styrene Induced by Monomers

model compound	$[\alpha]_{365}^{25}$ (deg) [a]	monomer	$[\alpha]_{365}^{25}$ (deg) [a]	polymer	$[\alpha]_{365}^{25}$ (deg) [a]	$[\theta]_{306} \times 10^{-3}$ (deg cm^2 dmol^{-1}) [b]	parity [c]	helical sense of induced N* [d]	β_M (μm^{-1})
***R*-(−)-HexI0**	−86.8	***R*-(−)-HexM0**	−84.4	***R*-(−)-HexP0**	234.7	6.05	odd	RH (rod)	1.39 ± 0.02
***S*-(+)-HexI0**	86.3	***S*-(+)-HexM0**	84.0	***S*-(+)-HexP0**	−233.2	−6.14	odd	LH (sol)	−1.40 ± 0.02
***S*-(+)-HexI1**	24.2	***S*-(+)-HexM1**	22.1	***S*-(+)-HexP1**	23.4	0.02	even	RH (sed)	1.58 ± 0.02
***S*-(+)-HexI2**	17.1	***S*-(+)-HexM2**	18.2	***S*-(+)-HexP2**	−21.8	−1.09	odd	LH (sol)	−1.62 ± 0.02
***S*-(+)-HexI3**	12.7	***S*-(+)-HexM3**	12.6	***S*-(+)-HexP3**	14.6	0.01	even	RH (sed)	0.96 ± 0.02
***R*-(−)-I0Hex**	−65.0	***R*-(−)-M0Hex**	−63.2	***R*-(−)-P0Hex**	282.4	8.32	odd	RH (rod)	5.43 ± 0.02
***S*-(+)-I0Hex**	64.8	***S*-(+)-M0Hex**	63.0	***S*-(+)-P0Hex**	−284.1	−8.33	odd	LH (sol)	−5.42 ± 0.02
***S*-(+)-I1Hex**	20.4	***S*-(+)-M1Hex**	18.1	***S*-(+)-P1Hex**	530.7	14.51	even	RH (sed)	1.96 ± 0.02
***S*-(+)-I2Hex**	17.3	***S*-(+)-M2Hex**	16.4	***S*-(+)-P2Hex**	−26.5	−1.25	odd	LH (sol)	−1.64 ± 0.02
***S*-(+)-I3Hex**	15.9	***S*-(+)-M3Hex**	14.6	***S*-(+)-P3Hex**	157.4	2.87	even	RH (sed)	1.00 ± 0.02

[a] Specific optical rotation in unit of degree was measured in a 1 dm cell at a concentration of ca. 5.0 mg/mL in THF at 25 °C. [b] Molecular ellipticity at 306 nm estimated from the CD spectra in Figure 2. [c] The position of the chiral center relative to *p*-terphenyl core. [d] Right-handed (RH) and left-handed (LH) helical senses determined based on Mauguin's model.[23]

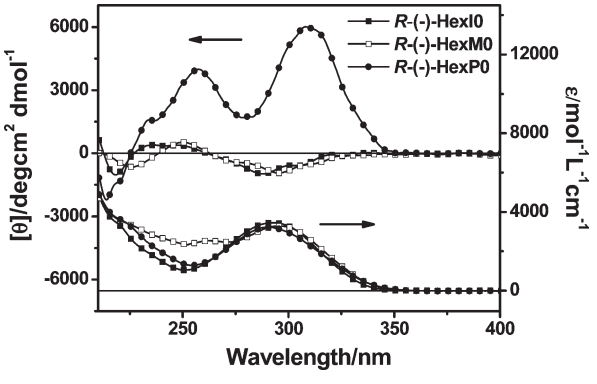

Figure 1. CD and UV−vis absorption spectra of ***R*-(−)-HexI0**, ***R*-(−)-HexM0**, and ***R*-(−)-HexP0** in THF at a concentration of 2 × 10^{-5} mol/L.

skewed way. Although the major electronic transitions of ***R*-(−)-HexI0** were essentially those of the polymer, its CD spectrum was quite like that of monomer, showing just weak Cotton effects in the wavelength range concerned. All the other polymers, with the exception of ***S*-(+)-HexP1** and ***S*-(+)-HexP3**, showed CD spectra distinct to their corresponding monomers and model compounds. On the basis of the chiroptical properties of polymers and their similar structures to the previously reported polymers,[22,24] the formation of helical conformation of polymer main chain was again proposed.

Odd−Even Effect. As indicated previously, an odd−even effect was found in the radical polymerization of ***S*-(+)-M*m*/*R*-(−)-M0**, i.e., the sign of optical rotations of the resultant polymers alternated when the stereocenter with identical configuration was sequentially moved away from the *p*-terphenyl. Moreover, the chirl induction power of stereocenter became less intensive with increasing its distance to *p*-terphenyl. ***S*-(+)-HexM*m*/*R*-(−)-HexM0** and ***S*-(+)-M*m*Hex/*R*-(−)-M0Hex** studied in the present work had similar structures with ***S*-(+)-M*m*/*R*-(−)-M0** except that one of the chiral alkoxycarbonyl terminal of the latter was replaced by achiral hexyloxy group. Careful analyses of the chiroptical properties of ***S*-(+)-HexPm/*R*-(−)-HexP0** and ***S*-(+)-PmHex/*R*-(−)-P0Hex** revealed several interesting chiral teleinduction characters. First, the sense of polymer optical rotation was determined by the configuration of stereocenter and the distance between the stereocenter and *p*-terphenyl rather the distance of the stereocenter relative to the main-chain. Second, varying the parity of covalent bond number between stereocenter and *p*-terphenyl alternated the sign of the optical rotation of ***S*-(+)-PmHex, *S*-(+)-HexP0** and ***S*-(+)-HexP2**, although no chiral induction was observed in ***S*-(+)-HexP1** and ***S*-(+)-HexP3**. Next, the stereogenic center at the ortho position of vinyl group showed stronger induction power than that at the meta position.

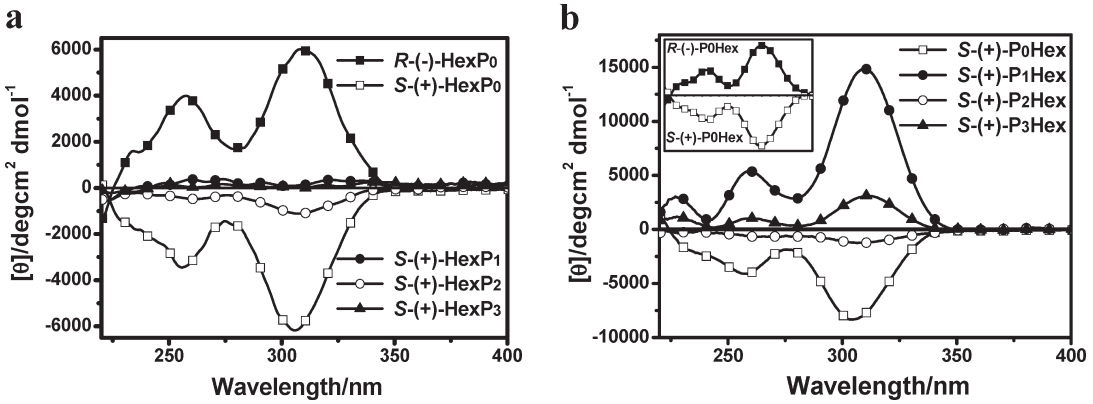

Figure 2. CD spectra of ***S*-(+)-HexPm**/***R*-(−)-HexP0** (a) and ***S*-(+)-PmHex**/***R*-(−)-P0Hex** (b) in THF at a Concentration of 2×10^{-5} mol/L.

Last, the chiral induction power of stereogenic center diminished in an odd−even way as it was away from the *p*-terphenyl core.

Figure 2 shows the CD spectra of ***S*-(+)-HexPm**/***R*-(−)-HexP0** and ***S*-(+)-PmHex**/***R*-(−)-P0Hex**. All these polymers exhibited intensive absorptions at about 296 nm. The polymer ***S*-(+)-P0Hex** had two intensive positive Cotton effects in the absorption region of *p*-terphenyl group. The other three analogous polymers, ***S*-(+)-P1Hex**, ***S*-(+)-P2Hex**, and ***S*-(+)-P3Hex**, also presented Cotton effects in the same region. However, their signs alternated and the intensities decreased in an odd−even way as the distance between the stereocenter and *p*-terphenyl increased. This was in accord with the optical rotation studies. The polymer ***R*-(−)-P0Hex** exhibited a mirror CD image to that of ***S*-(+)-P0Hex**, indicating enantiomeric conformations with opposite helicities adopted by the two polymers.

For the other five polymers with chiral terminals at the meta position of the vinyl group, only ***S*-(+)-HexP0**, ***S*-(+)-HexP0**, and ***R*-(−)-HexP2** displayed discernible Cotton effects centered at 306 and 255 nm, respectively. However, the strength was much weaker than their counterparts, ***S*-(+)-P0Hex**, ***S*-(+)-P2Hex**, and ***R*-(−)-P0Hex**, implying a reduced chiral induction power. In a stark contrast, the spectra of ***S*-(+)-HexP1** and ***S*-(+)-HexP3** show neglectable CD signals in the absorption region of the side groups, suggesting a poor asymmetric induction in the twisting sense preference of the polymer chain.

Liquid Crystal Induced Circular Dichroism. LCICD was employed to build the connection between the odd−even effects of the screw sense preferences in twisting mesophase and helical polymers.[18,22] The method was first developed by Serrano et al.,[18a] based on the study of optically active polyisocyanides derived from chiral premesogenic monomers, and was recently applied by us in study on radical polymerization of ***S*-(+)-M*m*** and ***R*-(−)-M0**.[22] It was considered that the steric influence of chiral tails influenced the diastereoselectivity of polymerization. Because some of ***S*-(+)-HexM*m*/*R*-(−)-HexM0** and ***S*-(+)-M*m*Hex/*R*-(−)-M0Hex** were not liquid crystalline, they were doped into an achiral liquid crystalline compound, 2,5-bis(4′-hexyloxyphenyl)styrene (**BHPSt**), which displays enantiotropic nematic phase in the temperature range from 64.1 to 85.5 °C.[22] **BHPSt** was selected as a host because its structure was closely similar to the monomers studied here, which favored noncovalent interaction of guest and host molecules. Figure 3 shows the texture of the mixture of ***R*-(−)-HexM0** and **BHPSt** (the textures of **BHPSt** doped with other monomers were presented in Supporting Information). All the monomers induced **BHPSt** to form chiral nematic phases and

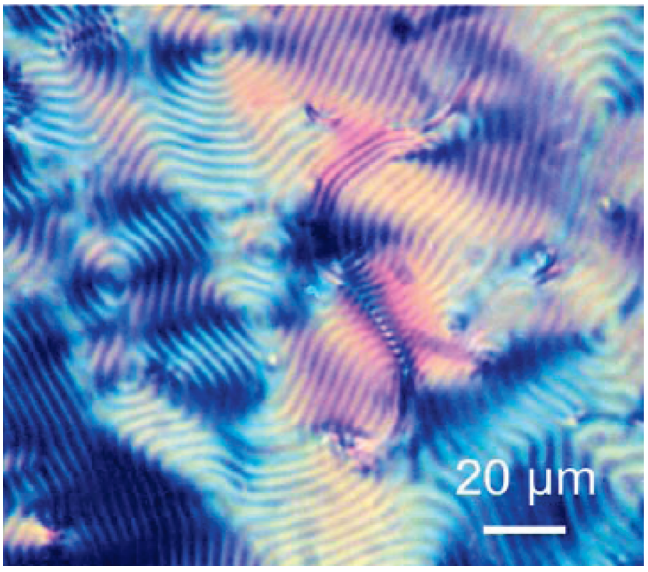

Figure 3. Fingerprint texture of cholesteric phase (p = 7.1 μm) of **BHPSt** doped with ***R*-(−)-HexM0** (10 wt %), taken under a cross-polarized optical microscope at 60 °C.

exhibited fingerprint textures with pitches of several micrometers. Figure 4 shows the CD spectra of cholesteric liquid crystal of **BHPSt** doped by chiral monomers. The intensive Cotton effects appeared in the wavelength range from 550 to 330 nm, remarkably less than the pitches of induced cholesteric mesophases. Therefore, the positive Cotton effects represented the presence of left-handed helix, while the negative signals indicated opposite one.[26] The results are collected in Table 2. When the parity of m in ***S*-(+)-HexM*m***** and ***S*-(+)-M*m*Hex** were odd, the N* phase of **BHPSt** induced by these molecules showed positive CD signal, suggesting left-handed (LH) long axis ordering, whereas the N* phase of **BHPSt** induced by the other monomers displayed negative CD signals, indicating right-handed ordering. Although the twisting directions of the corresponding polymer backbones remained unknown, the parallel in the odd−even effects between the helical sense of induced N* phase and the direction of optical rotation of the polymers was observed.

Role Governing Chiral Teleinduction. On the basis of these results, a chiral teleinduction mechanism in the radical polymerization of ***S*-(+)-HexM*m*/*R*-(−)-HexM0** and ***S*-(+)-M*m*Hex/*R*-(−)-M0Hex** was proposed by analogy with chiral promesogenic isocyanides and our previously reported bulky vinyl monomers ***S*-(+)-M*m*** and ***R*-(−)-M0**.[18b,22] The

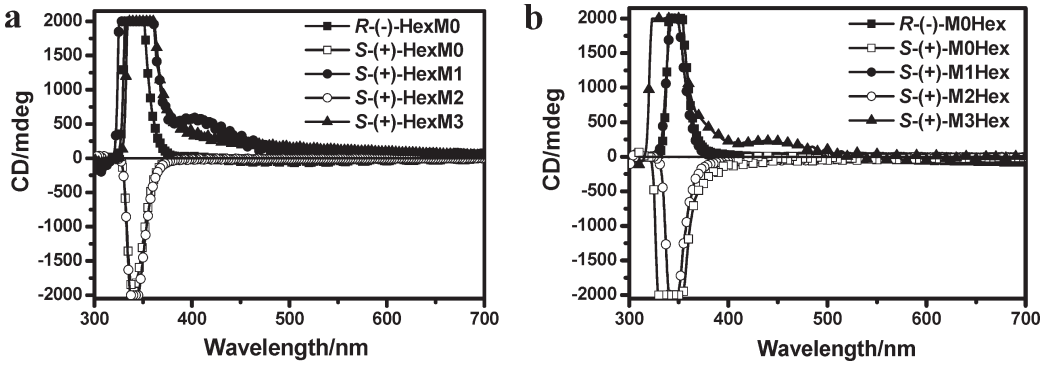

Figure 4. CD Spectra of induced cholesteric phase of **BHPSt** doped with ***S*-(+)-HexM*m*/*R*-(−)-HexM0** (a) and ***S*-(+)-M*m*Hex/*R*-(−)-M0Hex** (b) at 60 °C.

polymers from ***S*-(+)-HexM*m*/*R*-(−)-HexM0** and ***S*-(+)-M*m*Hex/*R*-(−)-M0Hex** consisted of flexible polyethylene backbones substituted with 4-hexyloxy-4′-alkoxycarboxyterphenyl group from waist or gravimetric position at every second carbon atom of the main chain. Such a unique macromolecular architecture owned a very large steric repulsion of highly crowded side group, which restricted the rotation around C−C bonds linking backbone carbons and gave rise to atropisomerism. *p*-Terphenyl, like phenyl benzoate in promesogenic isocyanides, helped long-range chirality transfer from stereogenic center in the side chain to the propagation main chain during polymerization.[18g,22] The asymmetry originated from the stereocenter in the monomer induced *p*-terphenyl to adopt a chiral conformation and as a result formed two differentiated diastereomeric faces in the proximity of the vinyl group. Driven by a similar noncovalent intermolecular interaction in induced cholesteric phases, the incoming monomer interacted stereoselectively with the growing species, leading to an excess of one screw sense in the resultant polymer. Changing the position of the stereocenter along the alkyl chains led to a change in the conformation of aromatic group relative to the flexible tail in an odd−even way. These gave the odd−even alternation in the preferences of the screw sense of the polymer chains and in the helices of the induced N* phases. Therefore, the sign of optical rotations of polymers was same once they contained stereogenic center with identical configuration and distance to terphenyl core no matter it is located at ortho or meta position.

Given this mechanism, the fact that the polymers resulted from ***S*-(+)-HexM*m*/*R*-(−)-HexM0** showed much stronger optical rotations than their countparts, ***S*-(+)-M*m*Hex/*R*-(−)-M0Hex** might be rationalized by their difference in twisting power (β_M) in inducing achiral **BHPSt** to generate a chiral nematic phase, i.e., the lower the β_M value the weaker the bias that the stereocenter provided to guide distereoselectivity of polymerization.[27,28] The twisting power of a chiral dopant in nematic liquid crystal is defined as[27b]

$$\beta_M = (pcr)^{-1}$$

where p is the pitch (μm), c is the concentration (mole of solute/mol of solution), and r is the enantiomeric purity of the dopant. This parameter is usually used to characterize the inducing abililty of a chiral dopant. The pitch of chiral nematic phase formed by **BHPSt** doped with a certain amount of ***S*-(+)-HexM*m*/*R*-(−)-HexM0** or ***S*-(+)-M*m*Hex/*R*-(−)-M0Hex** was measured with the Grandjean-Cano method.[29] With the assumption of $r = 100\%$, the β_M value of each monomer was estimated and is summarized in Table 2. It was evident that ***S*-(+)-HexM*m*/*R*-(−)-HexM0** exhibited larger β_M than ***S*-(+)-M*m*Hex/*R*-(−)-M0Hex** and the difference decreased as the stereocenter was far away from *p*-terphenyl. This was consistent with the previous observations in specific optical rotations and Cotton effects. The larger twisting power of ***S*-(+)-M*m*Hex/*R*-(−)-M0Hex** compared to ***S*-(+)-HexM*m*/*R*-(−)-HexM0** probably arose from the increased rotation barrier around the single bond linking the two related phenyl rings. This has been found in chiral biphenyl systems where the bond rotation was restricted and controlled by various bridge bonds.[28] Reducing the distance between the stereocenter and *p*-terphenyl had the similar effect. Although this speculation seemed to be reasonable when ***S*-(+)-M*m*Hex/*R*-(−)-M0Hex** and ***S*-(+)-HexM*m*/*R*-(−)-HexM0** were compared, inconsistency existed when comparison was made in the same series of monomers. ***S*-(+)-M0Hex** and ***S*-(+)-M2Hex** had β_M values of −5.42 and −1.64 μm^{-1}, respective, which were much larger than those of ***S*-(+)-M1Hex** (1.96 μm^{-1}) and ***S*-(+)-M3Hex** (1.00 μm^{-1}). However, the polymers derived from the latter two monomers exhibited several times larger optical rotations than the polymers from the former two monomers. This could also be found in ***S*-(+)-HexM1** and ***S*-(+)-HexM0**.

These observations implied a complex chiral teleinduction in the radical polymerization of bulky vinyl monomers. It seemed that the helical senses of polymers were dominated by the configuration of stereocenter and its relative position to the rigid *p*-terphenyl as in chiral mesophase. The intensities of optical rotations and Cotton effects were affected by a combination of factors such as the configuration, the distance to *p*-terphenyl, and the position relative to vinyl group of stereocenter. The mechanism is being explored.

Conclusion

Two series of chiral bulky vinyl monomers, ***S*-(+)-HexM*m*/*R*-(−)-HexM0** and ***S*-(+)-M*m*Hex/*R*-(−)-M0Hex**, with laterally attached *p*-terphenyl side group terminated by achiral *n*-hexyloxy and chiral alkoxycarbonyl substituents, separately, were prepared. All of them contained only a single asymmetric carbon atom. The monomers in the former group had vinyl group oriented toward hexyloxy group, while those in the latter group had vinyl group toward alkoxycarbonyl group. Such a structural design allowed one to systematically investigate the effects of configuration and position of chiral atom on the chiroptical property of the resultant polymer, especially to know whether the distance between stereocenter and *p*-terphenyl or that between stereocenter and vinyl group played a dominant role in the induction of chain helicity. On the basis of the results obtained from polarimetry, circular dichroism, and LCICD, it was found

that the stereogenic centers in these monomers were able to transmit their chiralities to the propagation polymer chains during free radical polymerization, with the exception of ***S*-(+)-HexM1** and ***S*-(+)-HexM3**. The sign of optical rotations of the resultant polymers in THF depended on the absolute spatial configuration of chiral atom and its position relative to *p*-terphenyl group. Inverting the spatial configuration of asymmetric center or changing the parity of covalent bond number between stereocenter and *p*-terphenyl alternated the direction of optical rotation of polymer. This phenomenon paralleled the dependence of the helical twist sense of the chiral nematic phase of achiral **BHPSt** induced by the analogous chiral monomers, implying the identical driving force for the formation of chiral mesophase and the chiral secondary structure of the polymer. In addition, the monomers with vinyl group oriented toward chiral terminal showed larger induction power in the formation of chiral secondary structure than those with polymerizable group toward achiral terminal.

Experimental Section

Material. 5-Bromo-2-iodotoluene (97%, Aldrich), *N*-bromosuccinimide (NBS, 99%, Aldrich), triphenylphosphine (PPh_3, 99%, Acros), tetrachloromethane (CCl_4, AR, Beijing Chemical Co.), *S*-(+)-*sec*-butanol (99%, Acros), *R*-(−)-*sec*-butanol (99%, Acros), *S*-(+)-2-methylbutan-1-ol (99%, Acros), *S*-(+)-3-methylpentan-1-ol (98%, TCI), *S*-(+)-4-methylhexyan-1-ol (98%, TCI), and aqueous formaldehyde (40%, AR, Beijing Chemical Co.) were used as purchased. Benzoyl peroxide (BPO, AR, Wuhan Chemical Co.) was recrystallized from methanol and dried under vacuum at room temperature. Tetrahydrofuran (THF, AR, Beijing Chemical Co.) was refluxed with sodium and distilled out just before use. Anisole (AR, Beijing Chemical Co.) was distilled out from calcium hydride. Tetrakis(triphenylphosphine)palladium(0) ($Pd(PPh_3)_4$) was prepared according to the literature[30] procedure and kept in a refrigerator under argon. 4-(Hexyloxy)phenylboronic acid and 4-methyloxycarbonyl)phenylboronic acid were prepared according to the literature procedure.[31] All other reagents and solvents were used as obtained unless otherwise specified.

Measurements. ^{1}H NMR and ^{13}C NMR spectra were obtained on Bruker ARX400 or Bruker ARX300 spectrometers. The chemical shifts were reported in ppm (δ) relative to tetramethylsilane. Elementary analysis was carried out on a GmbH Vario EL instrument. Mass spectrum was recorded on a Bruker Inc. BIFLEX III spectrometer. Infra-Red (IR) spectra were recorded on a Nicolet Magna-IR 750 Fourier transform infrared spectrometer. The number-average molecular weight (M_n), weight-average molecular weight (M_w), and polydispersity (M_w/M_n) of polymers were determined by a gel permeation chromatography (GPC) apparatus equipped with a Waters 2410 refractive-index detector and a Water 515 pump. Three Waters Styragel columns with a 10 mm bead size were connected in series. Their effective molecular weight ranges were 100−10,000 for Styragel HT2, 500−30000 for Styragel HT3, and 5000−600000 for Styragel HT4, separately. The pore sizes were 50, 100, and 1000 nm for Styragel HT2, HT3, and HT4, respectively. THF was employed as the eluent at a flow rate of 1.0 mL/min at 35 °C. All GPC curves were calibrated against a series of monodispersed polystyrene standards. Optical rotations were estimated with a JASCO Model P-1030 digital polarimeter using a water-jacketed 100 mm cell at 25 °C. The temperature of water bath was mediated with a PolyScience programmable temperature controller. UV−vis absorption measurements were run on a Varian Cary 1E UV−vis spectrometer. CD spectra were recorded on a JASCO J-810 spectrometer. The sample solution was thermostated at 25 °C. The light path length of the quartz cell used was 10 mm. The concentration was 2×10^{-5} mol/L and the solvent was THF. Thermogravimetric analysis (TGA) was performed on a TA Q600 instrument at a heating rate of 10 °C/min in nitrogen atmosphere. The thermal transitions of the polymers were detected using Perkin-Elmer Pyris I DSC with a mechanical refrigerator. Samples with a typical mass of 3−7 mg were encapsulated in sealed aluminum pans. To observe the glass transition of polymers clearly, all the polymeric samples were cooled at a cooling rate of 2 °C/min from +280 to −10 °C first.

Mesophase Formation and Characterization. Mesophase textures were examined on a Leica DML polarized light optical microscope (POM) with a Linkam TH-600PM hot stage. To measure the power and direction of the chiral monomers to induce a chiral nematic phase (N*), these compounds were doped into an achiral liquid crystalline compound, **BHPSt**, at a certain concentration of 10 wt % for ***R*-(−)-HexM0**, 12 wt % for ***S*-(+)-HexM0**, 13 wt % for ***S*-(+)-HexM1**, 15 wt % for ***S*-(+)-HexM2**, 22 wt % for ***S*-(+)-HexM3**, 7 wt % for ***R*-(−)-M0Hex**, 7 wt % for ***S*-(+)-M0Hex**, 13 wt % ***S*-(+)-M1Hex**, 15 wt % for ***S*-(+)-M2Hex**, and 22 wt % for ***S*-(+)-M3Hex**. The formation of cholesteric phases was characterized by the existence of fingerprint texture or oily streak texture between two untreated glass slides observed POM. The mixtures were heated to isotropic melt state and introduced into either a parallel rubbed LC cell (thickness: 5 μm) or a Grandjean−Cano LC cell[29] (thickness: 3 μm at one side and 120 μm at other sides; length: 10 mm) by capillary action. The former was used to determine the screw senses of mesophases by the method based on CD. The CD spectra of N* phases were recorded by placing the cell perpendicular to the direction of the source beam. The latter was used to detect the pitch values by means of the Grandjean−Cano method, which was based on the observation of the discontinuity lines that appeared under POM.

Synthesis. *2-(4′-Hexyloxyphenyl)-5-bromotoluene*. To a degassed mixture of 5-bromo-2-iodo-toluene (14.9 g, 50 mmol), 4-(hexyloxy)phenylboronic acid (12.2 g, 55 mmol), and $Pd(PPh_3)_4$ (0.42 g, 0.36 mmol) were added into a solution containing benzene (150 mL), ethanol (100 mL) and aqueous Na_2CO_3 solution (2 M, 200 mL) under a continuous stream of argon. The solution was vigorously stirred at reflux for 6 h. Afterward, the organic layer was separated and dried over anhydrous Na_2SO_4. The solvent was taken away under reduced pressure and the residue was purified by column chromatography on silica gel (dichloromethane/petroleum ether: 1/5 (v/v) as eluent) to give 13.2 g of product as a yellow liquid. Yield: 76%. ^{1}H NMR (300 MHz, $CDCl_3$, δ ppm): 0.91−0.92 (t, 3H; CH_3), 1.34−1.39 (m, 4H; CH_2CH_2), 1.40−1.52 (m, 2H; CH_2), 1.77−1.85 (m, 2H; CH_2), 2.26 (s, 3H, CH_3), 3.99−4.03 (m, 2H; CH_2), 6.94−6.98 (d, 2H; Ar), 7.08−7.11 (d, 1H; Ar), 7.18−7.22 (d, 2H; Ar), 7.34−7.34 (d, 1H; Ar), 7.42 (s, 1H; Ar). Anal. Calcd for $C_{19}H_{23}BrO$: C, 65.71; H, 6.68. Found: C, 65.62; H, 6.91. MS: m/e = 346 (100%) and 348 (97%) (calcd 347.29).

2-(4′-Hexyloxyphenyl)-5-bromostyrene. A solution of 2-(4′-hexyloxyphenyl)-5-bromotoluene (10.41 g, 30 mmol), NBS (5.34 g, 30 mmol), and BPO (0.10 g, 0.4 mmol) in CCl_4 (180 mL) was refluxed for 3 h. After the reaction had cooled to room temperature, the solids suspended on the surface of the reaction mixture were separated by filtration. After evaporation of solvent under vacuum, yellow solids were obtained and were directly mixed with PPh_3 (7.88 g, 30 mmoL) and acetone (180 mL). The mixture was heated to reflux for 4 h. Afterward, the solvent was evaporated out under reduced pressure and the residue was purified by column chromatography on silica gel using dichloromethane at first and then methanol as eluent. The methanol phase was collected. After the removal of methanol, the residue was dissolved in aqueous formaldehyde (40 wt %, 180 mL). With a rapid stirring, aqueous NaOH solution (2.5 M, 100 mL) was dropped slowly at room temperature. The mixture was stirred for 24 h. When the reaction was completed, 3 × 150 mL potions of CH_2Cl_2 were used to extract the mixture. The organic layers were combined and dried over anhydrous Na_2SO_4. The solvent was taken away under reduced pressure

and the residue was purified by column chromatography on silica gel (dichloromethane/petroleum ether: 1/3 (v/v) as eluent) to give 7.76 g of yellow solids. Yield: 72%. ^{1}H NMR (300 MHz, CDC1$_3$, δ ppm): 0.89−0.91 (t, 3H, CH_3), 1.32−1.37 (m, 4H; CH_2CH_2), 1.43−1.50 (m, 2H; CH_2), 1.75−1.82 (m, 2H; CH_2), 3.96−4.00 (m, 2H; CH_2), 5.20−5.24 (d, 1H; vinyl), 5.65−5.71 (d, 2H; vinyl); 6.59−6.69 (q, 1H; vinyl); 6.91−6.94 (d, 2H; Ar), 7.11−7.14 (d, 1H; Ar), 7.18−7.22 (d, 2H; Ar), 7.39−7.42 (d, 1H; Ar), 7.73 (s, 1H; Ar). Anal. Calcd for $C_{20}H_{23}BrO$: C, 66.86; H, 6.45. Found: C, 66.67; H, 6.50. MS: m/e = 358 (100%) and 360 (97%) (calcd 359.3).

2-(4′-Hexyloxyphenyl)-5-(4′-methoxycarbonylphenyl)styrene. To a degassed mixture of 2-(4′-hexyloxyphenyl)-5-bromostyrene (7.18 g, 20 mmol), 4-(methoxycarbonyl)phenylboronic acid (3.96 g, 22 mmol), hydroquinone (0.22 g, 2 mmol) and Pd-(PPh_3)$_4$ (0.42 g, 0.36 mmol) were added benzene (74 mL), ethanol (54 mL) and aqueous $NaHCO_3$ solution (2 mol/L, 108 mL) under a continuous stream of argon. The solution was vigorously stirred at reflux for 6 h under argon. Afterward, the organic layer was separated and dried over anhydrous Na_2SO_4. The solvent was removed under reduced pressure and the residue was washed by petroleum to give 7.75 g of yellow solids, which were used directly in the following reaction without further purification. Yield: 94%. ^{1}H NMR (300 MHz, CDC1$_3$, δ ppm): 0.90−0.92 (t, 3H, CH_3), 1.33−1.37 (m, 4H; CH_2CH_2), 1.45−1.50 (m, 2H; CH_2), 1.77−1.85 (m, 2H; CH_2), 3.96 (s, 3H, OCH_3) 4.00−4.04 (m, 2H; CH_2), 5.25−5.28 (d, 1H; vinyl), 5.76−5.82 (d, 2H; vinyl); 6.76−6.86 (q, 1H; vinyl); 6.96−6.99 (d, 2H; Ar), 7.30−7.33 (d, 2H; Ar), 7.38−7.41 (d, 1H; Ar), 7.57−7.60 (d, 1H; Ar), 7.72−7.75 (d, 2H, Ar), 7.87 (s, 1H; Ar), 8.13−8.16 (d, 2H; Ar). Anal. Calcd for $C_{28}H_{30}O_3$: C, 81.13; H, 7.29. Found: C, 81.11; H, 7.32. MS: m/e = 414 (calcd 414.54).

2-(4′-Hexyloxyphenyl)-5-(4′-carboxylphenyl)styrene. To a solution of 2-(4′-hexyloxyphenyl)-5-(4′-methoxycarbonylphenyl)-styrene (7.0 g, 17 mmol) in THF (100 mL) and MeOH (100 mL) was added aqueous NaOH solution (2.5 M, 200 mL). The mixture was then vigorously stirred at reflux for 12 h. After addition of dichloromethane (400 mL), the mixture was acidified by hydrochloric acid (37 wt %) to give aqueous phase with a pH value of 2. The organic layer was separated and dried over anhydrous Na_2SO_4. The solvent was removed under reduced pressure to provide 6.52 g of target product. Yield: 96%. ^{1}H NMR (400 MHz, DMSO-d_6, δ ppm): 0.87−0.91 (t, 3H, CH_3), 1.31−1.35 (m, 4H; CH_2CH_2), 1.41−1.47 (m, 2H; CH_2), 1.70−1.77 (m, 2H; CH_2), 4.00−4.03 (m, 2H; CH_2), 5.24−5.27 (d, 1H; vinyl), 5.74−5.79 (d, 1H; vinyl), 6.76−6.90 (q, 1H; vinyl), 6.99−7.02 (d, 2H; Ar), 7.29−7.31 (d, 2H; Ar), 7.37−7.40 (d, 1H; Ar), 7.58−7.60 (d, 1H; Ar), 7.71−7.74 (d, 2H, Ar), 7.85 (s, 1H; Ar), 8.10−8.13 (d, 2H; Ar). Anal. Calcd for $C_{27}H_{28}O_3$: C, 80.97; H, 7.05. Found: C, 80.56; H, 7.37. MS: m/e = 400 (calcd 400.5).

(+)-2-(4′-Hexyloxyphenyl)-5-(4′-(S)-sec-butyloxycarbonylphenyl)styrene (***S*-(+)-HexM0**). A mixture of 2-(4′-hexyloxyphenyl)-5-(4′-carboxylphenyl)styrene (0.5 g, 1.25 mmol) and oxalyl chloride (1.27 g, 10 mmol) in toluene (10 mL) was stirred at room temperature for 24 h. Afterward, the solvent was removed under reduced pressure and the residue was dissolved in dried THF (5 mL). With a rapid stirring, the solution was dropped slowly into a mixture of *S*-(+)-*sec*-butanol (0.1 g, 1.35 mmol) and pyridine (0.5 g, 6.3 mmol) in THF (5 mL) at 0 °C. The mixture was stirred for 2 h and then was poured into hydrochloric acid solution (2 mol/L, 100 mL). The mixture was extracted by 3 × 50 mL potions of CH_2Cl_2. The organic layers were combined and dried over anhydrous Na_2SO_4. The solvent was taken away under reduced pressure and the residue was purified by column chromatography on silica gel (dichloromethane/petroleum ether: 1/1 (v/v) as eluent) to give 0.21 g of product as white solids. Yield: 37%. ^{1}H NMR (400 MHz, $CDCl_3$, δ ppm): 0.90−0.94 (t, 3H, CH_3), 0.98−1.02 (t, 3H, CH_3), 1.31−1.37 (m, 7H; CH_2CH_2 and CH_3), 1.46−1.51 (m, 2H; CH_2), 1.66−1.85 (m, 4H; CH_2 and CH_2), 4.00−4.03 (t, 2H; CH_2), 5.11−5.16 (m, 1H, CH), 5.24−5.27 (d, 1H; vinyl), 5.75−5.80 (d, 1H; vinyl), 6.76−6.84 (q, 1H; vinyl), 6.95−6.98 (d, 2H; Ar), 7.29−7.32 (d, 2H; Ar), 7.37−7.39 (d, 1H; Ar), 7.55−7.58 (dd, 1H; Ar), 7.71−7.73 (d, 2H; Ar), 7.86 (s, 1H; Ar), 8.13−8.15 (d, 2H; Ar). ^{13}C NMR (100 MHz, CDC1$_3$, δ ppm): 9.79, 13.97, 19.62, 22.59, 25.72, 28.94, 29.23, 31.56, 67.99, 72.93 (10C, alkyl), 115.06, 136.02 (2C, CH═CH_2), 113.97, 114.16, 124.73, 126.45, 126.87, 129.64, 130.74, 130.85, 132.23, 136.32, 138.78, 140.32, 145.08, and 158.50 (18C, *p*-terphenyl), 166.07 (1C, C═O). Anal. Calcd for $C_{31}H_{36}O_3$: C, 81.54; H, 7.95. Found: C, 81.32; H, 7.98. MS: m/e = 456 (calcd 456.62). Specific optical rotation $[\alpha]_{365}^{25}$ = +84.0° (c 5 mg/mL, THF).

(−)-2-(4′-Hexyloxyphenyl)-5-(4′-(R)-sec-butyloxycarbonylphenyl)styrene (***R*-(−)-HexM0**). ^{1}H NMR (400 MHz, $CDCl_3$, δ ppm): 0.90−0.94 (t, 3H, CH_3), 0.98−1.02 (t, 3H, CH_3), 1.31−1.37 (m, 7H; CH_2CH_2 and CH_3), 1.46−1.51 (m, 2H; CH_2), 1.66−1.85 (m, 4H; CH_2 and CH_2), 3.99−4.03 (t, 2H; CH_2), 5.11−5.156 (m, 1H, CH), 5.24−5.27 (d, 1H; vinyl), 5.75−5.80 (d, 1H; vinyl), 6.76−6.83 (q, 1H; vinyl), 6.95−6.97 (d, 2H; Ar), 7.29−7.32 (d, 2H; Ar), 7.37−7.39 (d, 1H; Ar), 7.55−7.58 (dd, 1H; Ar), 7.71−7.73 (d, 2H; Ar), 7.85 (s, 1H; Ar), 8.13−8.15 (d, 2H; Ar). Anal. Calcd for $C_{31}H_{36}O_3$: C, 81.54; H, 7.95. Found: C, 81.50; H, 7.96. MS: m/e = 456 (calcd 456.62). Specific optical rotation $[\alpha]_{365}^{25}$ = −84.4° (c 5 mg/mL, THF).

(+)-2-(4′-Hexyloxyphenyl)-5-(4′-((S)-2-methylbutyloxy)carbonylphenyl)styrene (***S*-(+)-HexM1**). ^{1}H NMR (400 MHz, $CDCl_3$, δ ppm): 0.89−0.94 (t, 3H, CH_3), 0.96−1.00 (t, 3H, CH_3), 1.03−1.05 (d, 3H, CH_3), 1.33−1.47 (m, 8H; $CH_2CH_2CH_2$ and CH_2), 1.76−1.95 (m, 3H; CH_2 and CH), 3.99−4.03 (t, 2H; CH_2), 4.14−4.26 (ddd, 2H, CH_2), 5.24−5.27 (d, 1H; vinyl), 5.75−5.80 (d, 1H; vinyl), 6.76−6.84 (q, 1H; vinyl), 6.95−6.97 (d, 2H; Ar), 7.29−7.32 (d, 2H; Ar), 7.37−7.39 (d, 1H; Ar), 7.55−7.58 (dd, 1H; Ar), 7.71−7.73 (d, 2H; Ar), 7.86 (s, 1H; Ar), 8.13−8.15 (d, 2H; Ar). Anal. Calcd for $C_{32}H_{38}O_3$: C, 81.66; H, 8.14. Found: C, 81.46; H, 8.25. MS: m/e = 470 (calcd 470.64). Specific optical rotation $[\alpha]_{365}^{25}$ = +22.1° (c 5 mg/mL, THF).

(+)-2-(4′-Hexyloxyphenyl)-5-(4′-((S)-3-methylpentyloxy)carbonylphenyl)styrene (***S*-(+)-HexM2**). ^{1}H NMR (400 MHz, $CDCl_3$, δ ppm): 0.88−0.94 (m, 6H, CH_3 and CH_3), 0.97−0.98 (d, 3H, CH_3), 1.24−1.61 (m, 9H; $CH_2CH_2CH_2$ and $CHCH_2$), 1.78−1.87 (m, 4H; CH_2 and CH_2), 3.99−4.02 (t, 2H; CH_2), 4.37−4.42 (m, 2H, CH_2), 5.24−5.27 (d, 1H; vinyl), 5.75−5.80 (d, 1H; vinyl), 6.76−6.84 (q, 1H; vinyl), 6.95−6.97 (d, 2H; Ar), 7.29−7.32 (d, 2H; Ar), 7.37−7.39 (d, 1H; Ar), 7.55−7.58 (dd, 1H; Ar), 7.71−7.73 (d, 2H; Ar), 7.86 (s, 1H; Ar), 8.13−8.15 (d, 2H; Ar). Anal. Calcd for $C_{33}H_{40}O_3$: C, 81.78; H, 8.32. Found: C, 81.61; H, 8.44. MS: m/e = 484 (calcd 484.67). Specific optical rotation $[\alpha]_{365}^{25}$ = +18.2° (c 5 mg/mL, THF).

(+)-2-(4′-Hexyloxyphenyl)-5-(4′-((S)-4-methylhexyloxy)carbonylphenyl)styrene (***S*-(+)-HexM3**). ^{1}H NMR (400 MHz, $CDCl_3$, δ ppm): 0.87−0.94 (m, 9H, CH_3, CH_3, and CH_3), 1.15−1.51 (m, 11H; $CH_2CH_2CH_2$ and CH_2CHCH_2), 1.75−1.85 (m, 4H; CH_2 and CH_2), 3.99−4.03 (t, 2H; CH_2), 4.32−4.35 (m, 2H, CH_2), 5.24−5.27 (d, 1H; vinyl), 5.76−5.80 (d, 1H; vinyl), 6.76−6.83 (q, 1H; vinyl), 6.95−6.97 (d, 2H; Ar), 7. 30−7.32 (d, 2H; Ar), 7.37−7.39 (d, 1H; Ar), 7.56−7.58 (dd, 1H; Ar), 7.71−7.73 (d, 2H; Ar), 7.85 (s, 1H; Ar), 8.12−8.14 (d, 2H; Ar). Anal. Calcd for $C_{34}H_{42}O_3$: C, 81.89; H, 8.49. Found: C, 81.73; H, 8.60. MS: m/e = 498 (calcd 498.7). Specific optical rotation $[\alpha]_{365}^{25}$ = +12.6° (c 5 mg/mL, THF).

The monomers with vinyl group oriented toward chiral terminal were prepared in a similar way and the characterization data were summarized below.

2-(4′-Methoxycarbonylphenyl)-5-bromotoluene. Yield: 64%. ^{1}H NMR (300 MHz, $CDCl_3$, δ ppm): 2.23 (s, 3H, CH_3), 3.95 (s, 3H; CH_3), 7.06−7.11 (d, 1H; Ar), 7.34−7.44 (m, 3H; Ar), 7.44 (s, 1H; Ar), 8.01−8.11 (d, 1H; Ar). Anal. Calcd for $C_{15}H_{13}O_2$: C, 59.04; H, 4.29. Found: C, 59.03; H, 4.33. MS: m/e = 304 (100%) and 306 (97%) (calcd 305.17).

2-(4′-Methoxycarbonylphenyl)-5-bromostyrene. Yield: 56%. ^{1}H NMR (300 MHz, $CDCl_3$, δ ppm): 3.95 (s, 3H; CH_3), 5.30−5.34 (d, 1H; vinyl), 5.94−5.99 (d, 1H; vinyl), 6.60−6.70 (q, 1H; vinyl), 7.06−7.10 (d, 2H; Ar), 7.34−7.43 (m, 3H; Ar), 7.45 (s, 1H; Ar), 8.01−8.11 (d, 1H; Ar). Anal. Calcd for $C_{16}H_{13}O_2$: C, 60.59; H, 4.13. Found: C, 60.71; H, 4.03. MS: m/e = 316 (100%) and 318 (97%) (calcd 317.18).

2-(4′-Carboxylphenyl)-5-(4′-hexyloxyphenyl)styrene. Yield: 74%. ^{1}H NMR (300 MHz, DMSO-d_6, δ ppm): 0.87−0.91 (t, 3H, CH_3), 1.31−1.34 (m, 4H; CH_2CH_2), 1.39−1.44 (m, 2H; CH_2), 1.69−1.76 (m, 2H; CH_2), 4.00−4.04 (t, 2H; CH_2), 5.30−5.34 (d, 1H; vinyl), 5.94−5.99 (d, 1H; vinyl), 6.60−6.70 (q, 1H; vinyl), 7.03−7.06 (d, 2H; Ar), 7.37−7.39 (d, 1H; Ar), 7.47−7.49 (d, 2H; Ar), 7.63−7.66 (d, 1H; Ar), 7.69−7.72 (d, 2H, Ar), 7.91 (s, 1H; Ar), 8.02−8.04 (d, 2H; Ar). Anal. Calcd for $C_{27}H_{28}O_3$: C, 80.97; H, 7.05. Found: C, 80.61; H, 7.43. MS: m/e = 400 (calcd 400.5).

(+)-*2-(4′-(S)-sec-Butyloxycarbonylphenyl)-5-(4′-hexyloxyphenyl)styrene* (***S*-(+)-*M0Hex***). ^{1}H NMR (400 MHz, $CDCl_3$, δ ppm): 0.88−0.94 (m, 6H, CH_3), 0.98−1.02 (t, 3H, CH_3), 1.35−1.37 (m, 7H; CH_2CH_2 and CH_3), 1.45−1.50 (m, 2H; CH_2), 1.69−1.85 (m, 4H; CH_2 and CH_2), 3.99−4.03 (t, 2H; CH_2), 5.11−5.16 (m, 1H, CH), 5.24−5.27 (d, 1H; vinyl), 5.76−5.80 (d, 1H; vinyl), 6.68−6.75 (q, 1H; vinyl), 6.99−7.01 (d, 2H; Ar), 7.33−7.35 (d, 1H; Ar), 7.45−7.47 (d, 2H; Ar), 7.52−7.54 (dd, 1H; Ar), 7.57−7.59 (d, 2H; Ar), 7.81 (s, 1H; Ar), 8.09−8.12 (d, 2H; Ar). Anal. Calcd for $C_{31}H_{36}O_3$: C, 81.54; H, 7.95. Found: C, 81.32; H, 8.06. MS: m/e = 456 (calcd 456.62). Specific optical rotation $[\alpha]_{365}^{25}$ = +63.0° (c 5 mg/mL, THF).

(−)-*2-(4′-(R)-sec-Butyloxycarbonylphenyl)-5-(4′-hexyloxyphenyl)styrene* (***R*-(−)-*M0Hex***). ^{1}H NMR (400 MHz, $CDCl_3$, δ ppm): 0.90−0.94 (t, 3H, CH_3), 0.99−1.02 (t, 3H, CH_3), 1.34−1.38 (m, 7H; CH_2CH_2 and CH_3), 1.46−1.51 (m, 2H; CH_2), 1.69−1.84 (m, 4H; CH_2 and CH_2), 4.00−4.03 (t, 2H; CH_2), 5.11−5.16 (m, 1H, CH), 5.24−5.27 (d, 1H; vinyl), 5.76−5.80 (d, 1H; vinyl), 6.68−6.75 (q, 1H; vinyl), 6.99−7.01 (d, 2H; Ar), 7.34−7.36 (d, 1H; Ar), 7.45−7.48 (d, 2H; Ar), 7.53−7.55 (dd, 1H; Ar), 7.57−7.59 (d, 2H; Ar), 7.81 (s, 1H; Ar), 8.10−8.12 (d, 2H; Ar). Anal. Calcd for $C_{31}H_{36}O_3$: C, 81.54; H, 7.95. Found: C, 81.27; H, 8.06. MS: m/e = 456 (calcd 456.62). Specific optical rotation $[\alpha]_{365}^{25}$ = −63.2° (c 5 mg/mL, THF).

(+)-*2-(4′-((S)-2-Methylbutyloxy)carbonylphenyl)-5-(4′-hexyloxyphenyl)styrene* (***S*-(+)-*M1Hex***). ^{1}H NMR (400 MHz, $CDCl_3$, δ ppm): 0.91−0.94 (t, 3H, CH_3), 0.96−1.00 (t, 3H, CH_3), 1.03−1.05 (d, 3H, CH_3), 1.30−1.59 (m, 8H; $CH_2CH_2CH_2$ and CH_2), 1.78−1.90 (m, 3H; CH_2 and CH), 4.00−4.04 (t, 2H; CH_2), 4.15−4.27 (ddd, 2H, CH_2), 5.25−5.28 (d, 1H; vinyl), 5.76−5.81 (d, 1H; vinyl), 6.68−6.76 (q, 1H; vinyl), 6.99−7.02 (d, 2H; Ar), 7.34−7.36 (d, 1H; Ar), 7.45−7.49 (d, 2H; Ar), 7.53−7.55 (dd, 1H; Ar), 7.57−7.60 (d, 2H; Ar), 7.81 (s, 1H; Ar), 8.10−8.12 (d, 2H; Ar). Anal. Calcd for $C_{32}H_{38}O_3$: C, 81.66; H, 8.14. Found: C, 81.46; H, 8.25. MS: m/e = 470 (calcd 470.64). Specific optical rotation $[\alpha]_{365}^{25}$ = +18.1° (c 5 mg/mL, THF).

(+)-*2-(4′-((S)-3-Methylpentyloxy)carbonylphenyl)-5-(4′-hexyloxyphenyl)styrene* (***S*-(+)-*M2Hex***). ^{1}H NMR (400 MHz, $CDCl_3$, δ ppm): 0.91−0.95 (m, 6H, CH_3 and CH_3), 0.97−0.99 (d, 3H, CH_3), 1.24−1.61 (m, 9H; $CH_2CH_2CH_2$ and $CHCH_2$), 1.78−1.86 (m, 4H; CH_2 and CH_2), 4.00−4.04 (t, 2H; CH_2), 4.37−4.42 (m, 2H, CH_2), 5.24−5.27 (d, 1H; vinyl), 5.76−5.81 (d, 1H; vinyl), 6.70−6.78 (q, 1H; vinyl), 6.99−7.01 (d, 2H; Ar), 7.34−7.36 (d, 1H; Ar), 7.46−7.48 (d, 2H; Ar), 7.53−7.55 (dd, 1H; Ar), 7.58−7.60 (d, 2H; Ar), 7.81 (s, 1H; Ar), 8.09−8.11 (d, 2H; Ar). Anal. Calcd for $C_{33}H_{40}O_3$: C, 81.78; H, 8.32. Found: C, 81.74; H, 8.47. MS: m/e = 484 (calcd 484.67). Specific optical rotation $[\alpha]_{365}^{25}$ = +16.4° (c 5 mg/mL, THF).

(+)*2-(4′-((S)-4-Methylhexyloxy)carbonylphenyl)-5-(4′-hexyloxyphenyl)styrene* (***S*-(+)-*M3Hex***). ^{1}H NMR (400 MHz, $CDCl_3$, δ ppm): 0.87−0.94 (m, 9H, CH_3, CH_3, and CH_3), 1.17−1.51 (m, 11H; $CH_2CH_2CH_2$ and CH_2CHCH_2), 1.75−1.85 (m, 4H; CH_2 and CH_2), 4.00−4.03 (t, 2H; CH_2), 4.32−4.35 (m, 2H, CH_2), 5.24−5.27 (d, 1H; vinyl), 5.76−5.80 (d, 1H; vinyl), 6.68−6.75 (q, 1H; vinyl), 6.99−7.02 (d, 2H; Ar), 7.34−7.36 (d, 1H; Ar), 7.46−7.48 (d, 2H; Ar), 7.52−7.55 (dd, 1H; Ar), 7.56−7.60 (d, 2H; Ar), 7.81 (s, 1H; Ar), 8.09−8.11 (d, 2H; Ar).. Anal. Calcd for $C_{34}H_{42}O_3$: C, 81.89; H, 8.49. Found: C, 81.68; H, 8.64. MS: m/e = 498 (calcd 498.7). Specific optical rotation $[\alpha]_{365}^{25}$ = +14.6° (c 5 mg/mL, THF).

The model compounds were synthesized with a method similar to that used for the monomers.

(+)-*2-(4′-Hexyloxyphenyl)-5-(4′-(S)-sec-butyloxycarbonylphenyl)toluene* (***S*-(+)-*HexI0***). ^{1}H NMR (400 MHz, $CDCl_3$, δ ppm): 0.90−0.95 (t, 3H, CH_3), 0.98−1.02 (t, 3H, CH_3), 1.35−1.37 (m, 7H; CH_2CH_2 and CH_3), 1.45−1.52 (m, 2H; CH_2), 1.65−1.87 (m, 4H; CH_2 and CH_2), 2.37 (s, 3H, CH_3), 3.99−4.04 (t, 2H; CH_2), 5.10−5.16 (m, 1H, CH), 6.96−6.99 (d, 2H; Ar), 7.26−7.29 (d, 2H; Ar), 7.32−7.334 (d, 1H; Ar), 7.48−7.51 (dd, 1H; Ar), 7.54 (s, 1H; Ar), 7.68−7.72 (d, 1H; Ar), 8.13−8.15 (d, 2H; Ar). Anal. Calcd for $C_{30}H_{36}O_3$: C, 81.04; H, 8.16. Found: C, 80.80; H, 8.26. MS: m/e = 446 (calcd 446.62). Specific optical rotation $[\alpha]_{365}^{25}$ = +86.3° (c 5 mg/mL, THF).

(−)-*2-(4′-Hexyloxyphenyl)-5-(4′-(R)-sec-butyloxycarbonylphenyl)toluene* (***R*-(−)-*HexI0***). ^{1}H NMR (400 MHz, $CDCl_3$, δ ppm): 0.90−0.95 (t, 3H, CH_3), 0.98−1.02 (t, 3H, CH_3), 1.35−1.37 (m, 7H; CH_2CH_2 and CH_3), 1.45−1.52 (m, 2H; CH_2), 1.65−1.87 (m, 4H; CH_2 and CH_2), 2.37 (s, 3H, CH_3), 3.99−4.04 (t, 2H; CH_2), 5.10−5.16 (m, 1H, CH), 6.96−6.99 (d, 2H; Ar), 7.28−7.30 (d, 2H; Ar), 7.32−7.35 (d, 1H; Ar), 7.49−7.51 (dd, 1H; Ar), 7.54 (s, 1H; Ar), 7.69−7.72 (d, 1H; Ar), 8.12−8.15 (d, 2H; Ar). Anal. Calcd for $C_{30}H_{36}O_3$: C, 81.04; H, 8.16. Found: C, 80.80; H, 8.26. MS: m/e = 446 (calcd 446.62). Specific optical rotation $[\alpha]_{365}^{25}$ = −86.8° (c 5 mg/mL, THF).

(+)-*2-(4′-Hexyloxyphenyl)-5-(4′-((S)-2-methylbutyoxy)carbonylphenyl)toluene* (***S*-(+)-*HexI1***). ^{1}H NMR (400 MHz, $CDCl_3$, δ ppm): 0.90−1.00 (m, 6H, CH_3 and CH_3), 1.03−1.05 (d, 3H, CH_3), 1.26−1.56 (m, 8H; $CH_2CH_2CH_2$ and CH_2), 1.79−1.89 (m, 3H; CH_2 and CH), 2.37 (s, 3H, CH_3), 3.99−4.03 (t, 2H; CH_2), 4.14−4.26 (ddd, 2H, CH_2), 6.96−6.98 (d, 2H; Ar), 7.27−7.30 (d, 2H; Ar), 7.32−7.34 (d, 1H; Ar), 7.48−7.51 (dd, 1H; Ar), 7.53 (s, 1H; Ar), 7.69−7.72 (d, 1H; Ar), 8.12−8.15 (d, 2H; Ar). Anal. Calcd for $C_{31}H_{38}O_3$: C, 81.18; H, 8.35. Found: C, 81.07; H, 8.44. MS: m/e = 458 (calcd 458.63). Specific optical rotation $[\alpha]_{365}^{25}$ = +24.2° (c 5 mg/mL, THF).

(+)-*2-(4′-Hexyloxyphenyl)-5-(4′-((S)-3-methylpentyloxy)carbonylphenyl)toluene* (***S*-(+)-*HexI2***). ^{1}H NMR (400 MHz, $CDCl_3$, δ ppm): 0.88−0.94 (m, 6H, CH_3 and CH_3), 0.97−0.98 (d, 3H, CH_3), 1.24−1.61 (m, 9H; $CH_2CH_2CH_2$ and $CHCH_2$), 1.78−1.87 (m, 4H; CH_2 and CH_2), 2.36 (s, 3H, CH_3), 3.99−4.02 (t, 2H; CH_2), 4.37−4.43 (m, 2H, CH_2), 6.97−6.99 (d, 2H; Ar), 7.28−7.31 (d, 2H; Ar), 7.33−7.35 (d, 1H; Ar), 7.49−7.52 (dd, 1H; Ar), 7.54 (s, 1H; Ar), 7.70−7.73 (d, 1H; Ar), 8.13−8.16 (d, 2H; Ar). Anal. Calcd for $C_{32}H_{40}O_3$: C, 81.32; H, 8.53. Found: C, 81.21; H, 8.59. MS: m/e = 472 (calcd 472.66). Specific optical rotation $[\alpha]_{365}^{25}$ = +17.1° (c 5 mg/mL, THF).

(+)-*2-(4′-Hexyloxyphenyl)-5-(4′-((S)-4-methylhexyloxy)carbonylphenyl)toluene* (***S*-(+)-*HexI3***). ^{1}H NMR (400 MHz, $CDCl_3$, δ ppm): 0.88−0.94 (m, 9H, CH_3, CH_3, and CH_3), 1.16−1.52 (m, 11H; $CH_2CH_2CH_2$ and CH_2CHCH_2), 1.74−1.87 (m, 4H; CH_2 and CH_2), 2.38 (s, 3H, CH_3), 4.00−4.03 (t, 2H; CH_2), 4.32−4.36 (t, 2H, CH_2), 6.97−7.00 (d, 2H; Ar), 7.28−7.31 (d, 2H; Ar), 7.33−7.35 (d, 1H; Ar), 7.50−7.53 (dd, 1H; Ar), 7.5 (s, 1H; Ar), 7.71−7.73 (d, 1H; Ar), 8.13−8.16 (d, 2H; Ar). Anal. Calcd for $C_{33}H_{42}O_3$: C, 81.44; H, 8.70. Found: C, 81.24; H, 8.74. MS: m/e = 486 (calcd 486.68). Specific optical rotation $[\alpha]_{365}^{25}$ = +12.7° (c 5 mg/mL, THF).

(+)-*2-(4′-(S)-sec-Butyloxycarbonylphenyl)-5-(4′-hexyloxyphenyl)toluene* (***S*-(+)-*I0Hex***). ^{1}H NMR (400 MHz, $CDCl_3$, δ ppm): 0.91−0.95 (t, 3H, CH_3), 0.99−1.03 (t, 3H, CH_3), 1.35−1.38 (m, 7H; CH_2CH_2 and CH_3), 1.45−1.52 (m, 2H; CH_2), 1.65−1.87 (m, 4H; CH_2 and CH_2), 2.35 (s, 3H, CH_3), 4.00−4.03 (t, 2H; CH_2), 5.10−5.17 (m, 1H, CH), 6.98−7.00

(d, 2H; Ar), 7.28−7.30 (d, 1H; Ar), 7.44−7.49 (m, 4H; Ar), 7.55−7.57 (d, 2H; Ar), 8.10−8.12 (d, 2H; Ar). Anal. Calcd for $C_{30}H_{36}O_3$: C, 81.04; H, 8.16. Found: C, 81.00; H, 8.20. MS: m/e = 446 (calcd 446.62). Specific optical rotation $[\alpha]_{365}^{25}$ = +64.8° (c 5 mg/mL, THF).

(−)-*2-(4′-(R)-sec-Butyloxycarbonylphenyl)-5-(4′-hexyloxyphenyl)toluene* (***R*-(−)-*I0Hex***). ^{1}H NMR (400 MHz, $CDCl_3$, δ ppm): 0.91−0.95 (t, 3H, CH_3), 0.99−1.03 (t, 3H, CH_3), 1.35−1.38 (m, 7H; CH_2CH_2 and CH_3), 1.45−1.52 (m, 2H; CH_2), 1.65−1.87 (m, 4H; CH_2 and CH_2), 2.35 (s, 3H, CH_3), 4.00−4.03 (t, 2H; CH_2), 5.10−5.17 (m, 1H, CH), 6.98−7.00 (d, 2H; Ar), 7.28−7.30 (d, 1H; Ar), 7.44−7.49 (m, 4H; Ar), 7.55−7.57 (d, 2H; Ar), 8.10−8.12 (d, 2H; Ar). Anal. Calcd for $C_{30}H_{36}O_3$: C, 81.04; H, 8.16. Found: C, 81.00; H, 8.20. MS: m/e = 446 (calcd 446.62). Specific optical rotation $[\alpha]_{365}^{25}$ = −65.0° (c 5 mg/mL, THF).

(+)-*2-(4′-((S)-2-Methylbutyoxy)carbonylphenyl)-5-(4′-hexyloxyphenyl)toluene* (***S*-(+)-*I1Hex***). ^{1}H NMR (400 MHz, $CDCl_3$, δ ppm): 0.90−0.94 (t, 3H, CH_3), 0.96−1.00 (t, 3H, CH_3), 1.03−1.05 (d, 3H, CH_3), 1.31−1.59 (m, 8H; $CH_2CH_2CH_2$ and CH_2), 1.78−1.90 (m, 3H; CH_2 and CH), 2.34 (s, 3H, CH3), 3.99−4.03 (t, 2H; CH_2), 4.16−4.26 (ddd, 2H, CH_2), 6.97−6.99 (d, 2H; Ar), 7.27−7.29 (d, 1H; Ar), 7.43−7.48 (m, 4H; Ar), 7.55−7.57 (d, 2H; Ar), 8.10−8.12 (d, 2H; Ar). Anal. Calcd for $C_{31}H_{38}O_3$: C, 81.18; H, 8.35. Found: C, 80.99; H, 8.51. MS: m/e = 458 (calcd 458.63). Specific optical rotation $[\alpha]_{365}^{25}$ = +20.4° (c 5 mg/mL, THF).

(+)-*2-(4′-((S)-3-Methylpentyoxy)carbonylphenyl)-5-(4′-hexyloxyphenyl)toluene* (***S*-(+)-*I2Hex***). ^{1}H NMR (400 MHz, $CDCl_3$, δ ppm): 0.90−0.95 (m, 6H, CH_3 and CH_3), 0.97−0.99 (d, 3H, CH_3), 1.24−1.61 (m, 9H; $CH_2CH_2CH_2$ and $CHCH_2$), 1.78−1.87 (m, 4H; CH_2 and CH_2), 2.34 (s, 3H, CH_3), 4.00−4.03 (t, 2H; CH_2), 4.37−4.43 (m, 2H, CH_2), 6.97−6.99 (d, 2H; Ar), 7.27−7.29 (d, 1H; Ar), 7.43−7.48 (m, 4H; Ar), 7.55−7.57 (d, 2H; Ar), 8.09−8.11 (d, 2H; Ar). Anal. Calcd for $C_{32}H_{40}O_3$: C, 81.32; H, 8.53. Found: C, 81.37; H, 8.56. MS: m/e = 472 (calcd 472.66). Specific optical rotation $[\alpha]_{365}^{25}$ = +17.3° (c 5 mg/mL, THF).

(+)-*2-(4′-((S)-4-Methylhexyloxy)carbonylphenyl)-5-(4′-hexyloxyphenyl)toluene* (***S*-(+)-*I3Hex***). ^{1}H NMR (400 MHz, $CDCl_3$, δ ppm): 0.87−0.94 (m, 9H, CH_3, CH_3, and CH_3), 1.16−1.51 (m, 11H; $CH_2CH_2CH_2$ and CH_2CHCH_2), 1.74−1.87 (m, 4H; CH_2 and CH_2), 2.34 (s, 3H, CH_3), 4.00−4.03 (t, 2H; CH_2), 4.32−4.35 (t, 2H, CH_2), 6.97−7.00 (d, 2H; Ar), 7.28−7.31 (d, 2H; Ar), 7.33−7.35 (d, 1H; Ar), 7.50−7.53 (dd, 1H; Ar), 7.5 (s, 1H; Ar), 7.71−7.73 (d, 1H; Ar), 8.13−8.16 (d, 2H; Ar). Anal. Calcd for $C_{33}H_{42}O_3$: C, 81.44; H, 8.70. Found: C, 81.22; H, 8.88. MS: m/e = 486 (calcd 486.68). Specific optical rotation $[\alpha]_{365}^{25}$ = +15.9° (c 5 mg/mL, THF).

Radical Polymerization. Take ***S*-(+)-HexM0** for example. ***S*-(+)-HexM0** (0.136 g, 0.30 mmol), BPO (0.16 mg, 0.001 mmol), and anisole (0.9 mL) were added into a reaction tube. After three freeze−pump−thaw cycles, the tube was sealed under vacuum and put into an oil bath thermostated at 90 °C for 20 h. After being cooled to room temperature, the tube was opened and the solution was diluted with THF (10 mL). The mixture was dropped into cold methanol (200 mL). The precipitates were collected by filtration and washed by methanol. After they were dried under vacuum at room temperature for 24 h, 0.11 g of white solids was obtained. Yield: 81%.

Acknowledgment. The financial support of the National Natural Science Foundation of China (Nos. 20674001, 20834001), the National Science Fund for Distinguished Young Scholars (No. 20325415) and the China Postdoctoral Science Foundation (No. 20080440249) are greatly appreciated.

Supporting Information Available: Figures showing fingerprint textures and polarized optical micrographs, and DCS curves of the polymers and monomers and a table of pitch of cholesteric phase of **BHPSt** doped with monomers. This material is available free of charge via the Internet at http://pubs.acs.org.

References and Notes

(1) Nakano, T.; Okamoto, Y. *Chem. Rev*. **2001**, *101*, 4013–4038.
(2) Gao, J. P.; Chen, J. P.; Wang, Z. Y. *J. Am. Chem. Soc*. **1995**, *117*, 5377–5378.
(3) (a) Green, M. M.; Peterson, N. C.; Sato, T.; Teramoto, A.; Cook, R.; Lifson, S. *Science* **1995**, *268*, 1860–1866. (b) Green, M. M.; Park, J.-W.; Sato, T.; Teramoto, A.; Lifson, S.; Selinger, R. L. B.; Selinger, J. V. *Angew. Chem., Int. Ed*. **1999**, *38*, 3138–3154.
(4) Rowan, A. E.; Nolte, R. J. M. *Angew. Chem., Int. Ed*. **1998**, *37*, 63–68.
(5) Lam, J. W. Y.; Tang, B. Z. *Acc. Chem. Res*. **2005**, *38*, 745–754.
(6) (a) Okamoto, Y.; Suzuki, K.; Ohta, K.; Hatada, K.; Yuki, H. *J. Am. Chem. Soc*. **1979**, *101*, 4763–4765. (b) Nakano, T.; Okamoto, Y.; Hatada, K. *J. Am. Chem. Soc*. **1992**, *114*, 1318–1329. (c) Okamoto, Y.; Nishikawa, M.; Nakano, T.; Yashima, E.; Hatada, K. *Macromolecules* **1995**, *28*, 5135–5138.
(7) (a) Yashima, E.; Matsushima, T.; Okamoto, Y. *J. Am. Chem. Soc*. **1995**, *117*, 11596–11597. (b) Yashima, E.; Nimura, T.; Matsushima, T.; Okamoto, Y. *J. Am. Chem. Soc*. **1996**, *118*, 9800–9801. (c) Yashima, E.; Maeda, K.; Okamoto, Y. *Nature* **1999**, *399*, 449–451. (d) Maeda, K.; Ishikawa, M.; Yashima, E. *J. Am. Chem. Soc*. **2004**, *126*, 15161–15166. (e) Hasegawa, T.; Morino, K.; Tanaka, Y.; Katagiri, H.; Furusho, Y.; Yashima, E. *Macromolecules* **2006**, *39*, 482–488.
(8) (a) Ishikawa, M.; Maeda, K.; Mitsutsuji, Y.; Yashima, E. *J. Am. Chem. Soc*. **2004**, *126*, 732–733. (b) Kajitani, T.; Okoshi, K.; Sakurai, S. i.; Kumaki, J.; Yashima, E. *J. Am. Chem. Soc*. **2006**, *128*, 708–709. (c) Kajitani, T.; Okoshi, K.; Yashima, E. *Macromolecules* **2008**, *41*, 1601–1611. (d) Wu, Z. Q.; Nagai, K.; Banno, M.; Okoshi, K.; Onitsuka, K.; Yashima, E. *J. Am. Chem. Soc*. **2009**, *131*, 6708–6718.
(9) (a) Pino, P.; Lorenzi, G. P. *J. Am. Chem. Soc*. **1960**, *82*, 4745–4747. (b) Pino, P.; Ciardelli, F.; Montagnoli, G.; Pieroni, O. *J. Polym. Sci., Part B: Polym. Lett*. **1967**, *5*, 307–311.
(10) (a) Schlitzer, D. S.; Novak, B. M. *J. Am. Chem. Soc*. **1998**, *120*, 2196–2197. (b) Tang, H. Z.; Lu, Y.; Tian, G.; Capracotta, M. D.; Novak, B. M. *J. Am. Chem. Soc*. **2004**, *126*, 3722–3723. (c) Tian, G.; Lu, Y.; Novak, B. M. *J. Am. Chem. Soc*. **2004**, *126*, 4082–4083. (d) Tang, H. Z.; Boyle, P. D.; Novak, B. M. *J. Am. Chem. Soc*. **2005**, *127*, 2136–2142.
(11) Cheuk, K. K. L.; Lam, J. W. Y.; Li, B. S.; Xie, Y.; Tang, B. Z. *Macromolecules* **2007**, *40*, 2633–2642.
(12) (a) Kamer, P. C. J.; Nolte, R. J. M.; Drenth, W. *J. Am. Chem. Soc*. **1988**, *110*, 6818–6825. (b) Cornelissen, J. J. L. M.; Donners, J. J. J. M.; de Gelder, R.; Graswinckel, W. S.; Metselaar, G. A.; Rowan, A. E.; Sommerdijk, N. A. J. M.; Nolte, R. J. M. *Science* **2001**, *293*, 676–680.
(13) (a) Green, M. M.; Jha, S. K. *Chirality* **1997**, *9*, 424–427. (b) Green, M. M.; Zanella, S.; Gu, H.; Sato, T.; Gottarelli, G.; Jha, S. K.; Spada, G. P.; Schoevaars, A. M.; Feringa, B.; Teramoto, A. *J. Am. Chem. Soc*. **1998**, *120*, 9810–9817. (c) Park, J. W.; Ediger, M. D.; Green, M. M. *J. Am. Chem. Soc*. **2000**, *123*, 49–56. (d) Jha, S. K.; Cheon, K.-S.; Green, M. M.; Selinger, J. V. *J. Am. Chem. Soc*. **1999**, *121*, 1665–1673. (e) Khatri, C. A.; Pavlova, Y.; Green, M. M.; Morawetz, H. *J. Am. Chem. Soc*. **1997**, *119*, 6991–6995. (f) Tang, K.; Green, M. M.; Cheon, K. S.; Selinger, J. V.; Garetz, B. A. *J. Am. Chem. Soc*. **2003**, *125*, 7313–7323. (g) Li, J.; Schuster, G. B.; Cheon, K. S.; Green, M. M.; Selinger, J. V. *J. Am. Chem. Soc*. **2000**, *122*, 2603–2612.
(14) Ute, K.; Hirose, K.; Kashimoto, H.; Hatada, K.; Vogl, O. *J. Am. Chem. Soc*. **1991**, *113*, 6305–6306.
(15) (a) Fujiki, M. *J. Am. Chem. Soc*. **1994**, *116*, 6017–6018. (b) Fujiki, M. *J. Am. Chem. Soc*. **1996**, *118*, 7424–7425. (c) Nakashima, H.; Fujiki, M.; Koe, J. R.; Motonaga, M. *J. Am. Chem. Soc*. **2001**, *123*, 1963–1969. (d) Fujiki, M.; Koe, J. R.; Motonaga, M.; Nakashima, H.; Terao, K.; Teramoto, A. *J. Am. Chem. Soc*. **2001**, *123*, 6253–6261. (e) Nakashima, H.; Koe, J. R.; Torimitsu, K.; Fujiki, M. *J. Am. Chem. Soc*. **2001**, *123*, 4847–4848.
(16) (a) Maxein, G.; Zentel, R. *Macromolecules* **1995**, *28*, 8438–8440. (b) Muller, M.; Zentel, R. *Macromolecules* **1996**, *29*, 1609–1617. (c) Mruk, R.; Zentel, R. *Macromolecules* **2001**, *35*, 185–192. (d) Mayer, S.; Maxein, G.; Zentel, R. *Macromolecules* **1998**, *31*, 8522–8525. (e) Maxein, G.; Mayer, S.; Zentel, R. *Macromolecules* **1999**, *32*, 5747–5754.

(17) (a) Hu, Q. S.; Vitharana, D.; Liu, G. Y.; Jain, V.; Wagaman, M. W.; Zhang, L.; Lee, T. R.; Pu, L. *Macromolecules* **1996**, *29*, 1082–1084. (b) Huang, W. S.; Hu, Q. S.; Zheng, X. F.; Anderson, J.; Pu, L. *J. Am. Chem. Soc.* **1997**, *119*, 4313–4314. (c) Hu, Q. S.; Huang, W. S.; Vitharana, D.; Zheng, X. F.; Pu, L. *J. Am. Chem. Soc.* **1997**, *119*, 12454–12464. (d) Hu, Q. S.; Vitharana, D.; Liu, G.; Jain, V.; Pu, L. *Macromolecules* **1996**, *29*, 5075–5082. (e) Ma, L.; Hu, Q. S.; Musick, K. Y.; Vitharana, D.; Wu, C.; Kwan, C. M. S.; Pu, L. *Macromolecules* **1996**, *29*, 5083–5090. (f) Zhang, H. C.; Pu, L. *Macromolecules* **2004**, *37*, 2695–2702.

(18) (a) Ramos, E.; Bosch, J.; Serrano, J. L.; Sierra, T.; Veciana, J. *J. Am. Chem. Soc.* **1996**, *118*, 4703–4704. (b) Amabilino, D. B.; Ramos, E.; Serrano, J. L.; Sierra, T.; Veciana, J. *J. Am. Chem. Soc.* **1998**, *120*, 9126–9134. (c) Amabilino, D. B.; Ramos, E.; Serrano, J. L.; Veciana, J. *Adv. Mater.* **1998**, *10*, 1001–1005. (d) Amabilino, D. B.; Serranob, J. L.; Veciana, J. *Chem. Commun.* **2004**, 322–324. (e) Amabilinoa, D. B.; Ramosa, E.; Serranob, J. L.; Sierrab, T.; Vecianaa, J. *Polymer* **2005**, *46*, 1507–1521. (f) Gomar-Nadal, E.; Veciana, J.; Rovira, C.; Amabilino, D. B. *Adv. Mater.* **2005**, *17*, 2095–2098. (g) Amabilino, D. B.; Serrano, J.-L.; Sierra, T.; Veciana, J. *J.Polym. Sci. Part A: Polym. Chem.* **2006**, *44*, 3161–3174.

(19) (a) Nakako, H.; Nomura, R.; Masuda, T. *Macromolecules* **2001**, *34*, 1496–1502. (b) Tabei, J.; Nomura, R.; Masuda, T. *Macromolecules* **2003**, *36*, 573–577. (c) Sanda, F.; Nishiura, S.; Shiotsuki, M.; Masuda, T. *Macromolecules* **2005**, *38*, 3075–3078. (d) Tabei, J.; Shiotsuki, M.; Sanda, F.; Masuda, T. *Macromolecules* **2005**, *38*, 5860–5867. (e) Tabei, J.; Nomura, R.; Sanda, F.; Masuda, T. *Macromolecules* **2004**, *37*, 1175–1179.

(20) Lermo, E. R.; Langeveld-Voss, B. M. W.; Janssen, R. A. J.; Meijer, E. W. *Chem. Commun.* **1999**, 791–792.

(21) (a) Egbe, D. A. M.; Ulbricht, C.; Orgis, T.; Carbonnier, B.; Kietzke, T.; Peip, M.; Metzner, M.; Gericke, M.; Birckner, E.; Pakula, T.; Neher, D.; Grummt, U. W. *Chem. Mater.* **2005**, *17*, 6022–6032. (b) Satrijo, A.; Swager, T. M. *Macromolecules* **2005**, *38*, 4054–4057.

(22) Zhi, J.; Zhu, Z.; Liu, A.; Cui, J.; Wan, X.; Zhou, Q. *Macromolecules* **2008**, *41*, 1594–1597.

(23) Berova, N.; Nakanish, K.; Woody, R. W. *Circular Dichroism: Principles and Applications*, 2nd ed.; Wiley-VCH: New York, 2000; pp 547−561.

(24) (a) Yu, Z.; Wan, X.; Zhang, H.; Chen, X.; Zhou, Q. *Chem. Commun.* **2003**, 974–975. (b) Liu, A.; Zhi, J.; Cui, J.; Wan, X.; Zhou, Q. *Macromolecules* **2007**, *40*, 8233–8243. (c) Cui, J.; Liu, A.; Zhi, J.; Zhu, Z.; Guan, Y.; Wan, X.; Zhou, Q. *Macromolecules* **2008**, *41*, 5245–5254. (d) Zhi, J.; Guan, Y.; Cui, J.; Liu, A.; Zhu, Z.; Wan, X.; Zhou, Q. *J. Polym. Sci., Part A: Polym. Chem.* **2009**, *47*, 2408–2421.

(25) (a) Dutta, A. K.; Misra, T. N.; Pal, A. J. *J. Phys. Chem.* **1994**, *98*, 12844–12848. (b) Geiger, H. C.; Perlstein, J.; Lachicotte, R. J.; Wyrozebski, K.; Whitten, D. G. *Langmuir* **1999**, *15*, 5606–5616.

(26) (a) Gray, G. W.; McDonnel, D. G. *Mol. Cryst. Liq. Cryst.* **1977**, *34*, 211–217. (b) Goodby, J. W. *Science* **1986**, *231*, 350–355.

(27) (a) Gottarelli, G.; Samori, B.; Fuganti, C.; Grasselli, P. *J. Am. Chem. Soc.* **1981**, *103*, 471–472. (b) Gottarelli, G.; Hibert, M.; Samori, B.; Solladie, G.; Spada, G. P.; Zimmermann, R. *J. Am. Chem. Soc.* **1983**, *105*, 7318–7321. (c) Naciri, J.; Spada, G. P.; Gottarelli, G.; Weiss, R. G. *J. Am. Chem. Soc.* **1987**, *109*, 4352–4357. (d) Gottarelli, G.; Samor, B.; Stremmenos, C.; Torre, G. *Tetrahedron* **1981**, *37*, 395–399.

(28) (a) Yang, K.; Campbell, B.; Birch, G.; Williams, V. E.; Lemieux, R. P. *J. Am. Chem. Soc.* **1996**, *118*, 9557–9561. (b) Lazar, C.; Wand, M. D.; Lemieux, R. P. *J. Am. Chem. Soc.* **2000**, *122*, 12586–12587. (c) Swansburg, S.; Buncel, E.; Lemieux, R. P. *J. Am. Chem. Soc.* **2000**, *122*, 6594–6600. (d) di Matteo, A.; Todd, S. M.; Gottarelli, G.; Solladie, G.; Williams, V. E.; Lemieux, R. P.; Ferrarini, A.; Spada, G. P. *J. Am. Chem. Soc.* **2001**, *123*, 7842–7851. (e) Maly, K. E.; Wand, M. D.; Lemieux, R. P. *J. Am. Chem. Soc.* **2002**, *124*, 7898–7899.

(29) Cano, R. *Bull. Soc. Fr. Mineral. Cristallogr.* **1968**, *20*, 911.

(30) Brandsma, L.; Vasilevsky, S. F.; Verkruijsse, H. D. *Application of transition metal catalysis in organic synthesis*; Springer: New York, 1999; p 5.

(31) (a) Zhu, Z.; Zhi, J.; Liu, A.; Cui, J.; Tang, H.; Qiao, W.; Wan, X.; Zhou, Q. *J. Polym. Sci., Part A: Polym. Chem.* **2007**, *45*, 830–847. (b) Yu, Z.; Tu, H.; Wan, X.; Chen, X.; Zhou, Q. F. *J. Polym. Sci., Part A: Polym. Chem.* **2003**, *41*, 1454–1464.